A Photon Counting Hot-Electron Bolometer for Space THz Spectroscopy

Boris S. Karasik, Andrei V. Sergeyev, David Olaya, Jian Wei, Michael E. Gershenson, Jonathan H. Kawamura, and William R. McGrath

***Abstract*—We discuss a concept of the hot-electron transition-edge sensor (TES) capable of counting THz photons. The main need for such a THz calorimeter is spectroscopy on future space telescopes with a background limited *NEP* ~ 10^{-20} W/Hz$^{1/2}$. The micromachined bolometers will unlikely reach such sensitivity at temperatures above 10 mK. The hot-electron TES with sufficient sensitivity will still have a time constant ~ 0.1-1.0 ms that is too short for integrating a flux of THz background photons arriving at a rate of < 100 s^{-1}. The Hot-Electron Photon Counter based on a submicron-size superconducting *Ti* bridge with *Nb* Andreev contacts will be able to detect individual photons above 170 GHz due to its very low heat capacity. A discrimination of the low energy fluctuations with a threshold device would allow for realization of an *NEP* ~ 10^{-20} W/Hz$^{1/2}$ at ≳ 1 THz while operating at 300 mK. With the sensor time constant of a few microseconds, the dynamic range is ~ 30-40 dB. A compact array of the antenna-coupled counters can be fabricated on a silicon wafer without membranes. The initial fabricaiton effort has been successful yielding nanodevices with desired characteristics, which are currently are being tested.**

***Index Terms*—radiation detectors, submillimeter wave detectors, bolometers, superconducting devices.**

I. Introduction

Several new advanced space submillimeter (SMM) astronomy missions (Single-Aperture FIR Observatory – SAFIR [1,2], Submillimeter Probe of the Evolution of Cosmic Structure – SPECS [3], Space Infrared Telescope for Cosmology and Astrophysics – SPICA [4]) have been recently proposed. They are expected to make a dramatic impact on the attainable sensitivity in the moderate resolution mode ($\nu/\Delta\nu \sim 1000$) where direct detectors are typically used. This will be achieved by active cooling of telescope mirrors to 4-5 K. For all existing platforms, the radiation of the atmosphere and/or the temperature of the telescope set the sensitivity limit. Deep cooling of a telescope mirror to ~4K would almost completely eliminate the effect of the telescope emissivity. Then the limiting noise equivalent power (*NEP*) would be set by the background fluctuation at the level of ~ 10^{-19}-10^{-20} W/Hz$^{1/2}$ in the most of the SMM range (see Fig. 1).

The required *NEP* is two-three orders of magnitude lower then that currently achieved by the state-of-the-art (SOA) micromachined bolometers. Although it has been speculated that more than an order of magnitude improvement of the performance could be achieved for SOA detectors [2,5], we show in Section II that the improvement of the bolometer sensitivity is restricted by the quantum limitations imposed on the phonon conductance in 1-D channels below 1 K.

Alternative approaches for achieving the *NEP* ~ 10^{-20} W/Hz$^{1/2}$ include a number of concepts, namely, a superconducting [6] or normal metal [7] hot-electron bolometer, a kinetic inductance detector [8,9], a superconducting tunnel-junction device with a single-electron transistor readout [10], a hot-spot superconducting detector [11], and quantum-dot devices [12]. Data of Fig. 1 show that the low *NEP* above 1 THz corresponds to a very low photon arrival rate $N_{ph} < 100$ s^{-1}. This makes integration of weak signals impossible for all perspective detector concepts. Indeed, the time constant cannot be easily engineered and is determined by either the electron-phonon relaxation time [6,7,11] or by the quasiparticle recombination time [8-10] which both are of the order of a few milliseconds at 100 mK where the low *NEP* can only be achieved (see Section III). This circumstance makes photon counting a preferable mode of operation, at least for

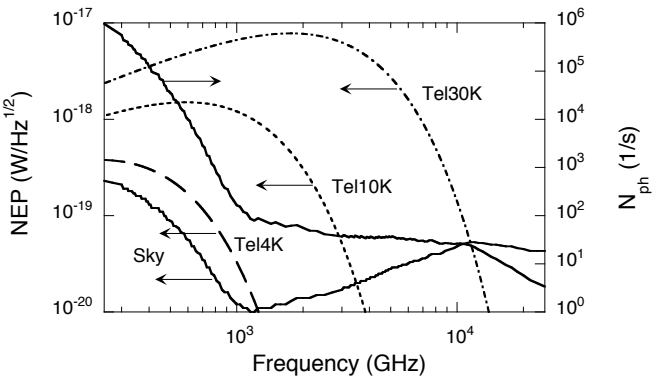

Fig. 1. The *NEP* limited by the background and by the telescope emission (5% emissivity, mirror temperature 4K, 10K, and 30K) for a moderate resolution spectrometer ($\nu/\Delta\nu = 1000$, single mode) and the rate of photon arrival from the background. The latter is less than 100 s^{-1} above 1 THz. Below 1 THz, the radiation originates from the Cosmic Microwave Background. At higher frequencies, the radiation from the galactic core and from the dust clouds dominates.

Boris S. Karasik (phone: +1-818-393-4438; fax: +1-818-393-4683; e-mail: boris.s.karasik@jpl.nasa.gov), Johathan H. Kawamura, and William R. McGrath are with the Jet Propulsion Laboratory, California Institute of Technology, Pasadena, CA 91109, USA.

Andrei V. Sergeyev is with the SUNY at Buffalo, Buffalo, NY 14260, USA.

David Olaya, Jian Wei and Michael E. Gershenson are with the Department of Physics and Astronomy of Rutgers University, 136 Frelinghuysen Rd., Piscataway, NJ 08854, USA.

The work of B.S.K., J.H.K. and W.R.M. was carried out at the Jet Propulsion Laboratory, California Institute of Technology, under a contract with the National Aeronautics and Space Administration and funded through the internal Research and Technology Development program.

The work of A.V.S. was supported by a NASA grant.

The work of D.O., J.W. and M.E.G. at Rutgers University was supported in part by the NASA grants NNG04GD55G and NAG5-10357 and the Rutgers Academic Excellence Fund.

detection of weak signals. The photon counting mode at SMM has been considered in [10] and [11]. The only experimental demonstration of the detection of single SMM photons has been done using quantum-dot devices [12]. However, the potential difficulties associated with coupling of radiation and with detector array readout make alternative approaches worth of pursuing.

In Section IV, we analyze the photon counting regime for a Hot-Electron Direct Detector (HEDD) [6], which is a transition-edge sensor (TES) operated in the hot-electron mode and whose sensitivity is enhanced due to the disorder-suppressed electron-phonon coupling [13]. The main advantage of the photon counting is that the *NEP* ~ 10^{-20} W/Hz$^{1/2}$ can be actually achieved at 300 mK instead of 100 mK that tremendously relieves the cryocooling problem for space applications.

In Seciton V, we present the current status of the device nanofabrication and testing.

II. Sensitivity Limit in Micromachnied Bolometers

Bolometers are currently detectors of choice for SMM astronomical instruments. The SOA design of a SMM bolometer represents a very fine mesh ("spider-web") etched from a 1-μm thick Si_3N_4 membrane that suspends a sensitive Neutron-Transmutation-Doped *Ge* (NTD-*Ge*) thermometer. The mesh plays simultaneously the role of the thermal conductance to the bath and of the radiation absorber. One of the most important applications of these bolometers will be the High-Frequency Instrument on the NASA/ESA Planck Surveyor Mission where a typical background-limited *NEP* ~ 10^{-17}-10^{-16} W/Hz$^{1/2}$ will be utilized in several frequency bands between 100 GHz and 857 GHz [14].

The fundamental *NEP* of a bolometer is set by the minimum possible thermal conductance between the absorber of radiation and the thermal sink. "Spider-web" bolometers use several (~10) 500 μm long, 1 μm thick and 3 μm wide Si_3N_4 legs, each of which contributes ~ 1 pW/K into the thermal conductance at 100 mK. The further decrease of the thermal conductance might be seen via change of the leg geometry and decrease of the number of legs assuming that the "classical" T^3-dependence of the thermal conductivity holds down to the lowest temperatures. There is, however, new data on the thermal conductance of dielectric nanowires setting some doubt about a realism of this approach. Theory [15], which takes into account the quantization of phonon modes in thin wires, gives the following low temperature ballistic transport limit for the thermal conductance:

$$G_Q = 4\pi^2 k_B^2 T / 3h = 3.8 \cdot T \quad [pW/K]. \tag{1}$$

Remarkably, this quantity does not depend on the length of the wire and on its material. The experiments with Si_3N_4 [16], *GaAs* wires [17] and nanotubes [18] confirm the theory demonstrating the crossover of the conductance from the T^3-dependence to the linear dependence of (1). Although the crossover temperature depends on the material purity, the lowest possible conductance is still given by (1). If we assume a hypothetical 4-leg isolated bolometer then the quantum conductance limited NEP_Q will be given by:

$$NEP_Q = \sqrt{4k_B T^2 \cdot 4G_Q} \tag{2}$$

At 100 mK, (2) yields an *NEP* which is slightly less than 10^{-18} W/Hz$^{1/2}$. It approaches the 10^{-20} W/Hz$^{1/2}$ only below 10 mK, which is an impractically low temperature for space instruments. Unless an efficient way for a drastic increase of the reflectivity for phonons entering the bolometer leg is figured out, the sensitivity of micromachined bolometers will be fundamentally limited by expression (2).

III. Relaxation Time and Operating Modes in Non-Equilibrium Sensors

Two actively pursued approaches to sensitive integrating SMM detectors are the HEDD [6] and the Kinetic Inductance Detector (KID) [9]. The time constant in those detectors cannot be engineered as readily as in micromachined bolometers and requires a special consideration.

The low background *NEP* corresponds to a low photon arrival rate:

$$N_{ph} = \frac{1}{2}\left(\eta \frac{NEP}{h\nu}\right)^2, \tag{3}$$

where η is the quantum efficiency. Above 1 THz, $N_{ph} < 100$ s^{-1} (see Fig. 1). A detector with a time constant τ will integrate photon flux if $N_{ph}\tau >> 1$. Therefore, a background limited integrating detector must have a time constant of 100 ms or greater. Such a long time constant is problematic for both KID and HEDD approaches.

The KID senses a number of Cooper pairs broken by photons. This causes a decrease of the kinetic inductance of a superconducting film that can be detected either by an inductive bridge with a SQUID [8] or via a shift of the resonance frequency in a strongly coupled microstrip resonator [9]. The fundamental sensitivity limit is set by the quasiparticle generation-recombination noise [8]:

$$NEP_{GR} = 2\Delta\sqrt{N_{qp}/\tau_{qp}}\,. \tag{4}$$

Here N_{qp} is the number of quasiparticles, τ_{qp} is the quasiparticle lifetime due to the recombination modified by phonon trapping effects in the film. In an *Al* sample [19], $N_{qp} \approx 10^4$ and $\tau_{qp} \approx 0.1$ ms have been realized at 0.2 K, thus yielding $NEP_{GR} \sim 10^{-19}$ W/Hz$^{1/2}$. Although, theoretically, τ_{qp} has strong exponential temperature dependence and could be very long at low temperatures, no value greater than 0.1 ms has been reported to date. Sometimes, a saturation of τ_{qp} is seen below some certain temperature [9].

The HEDD relies on a weak electron-phonon coupling in disordered *Hf* or *Ti* superconducting films. The fundamental noise limit is set by the thermal energy fluctuations (TEF):

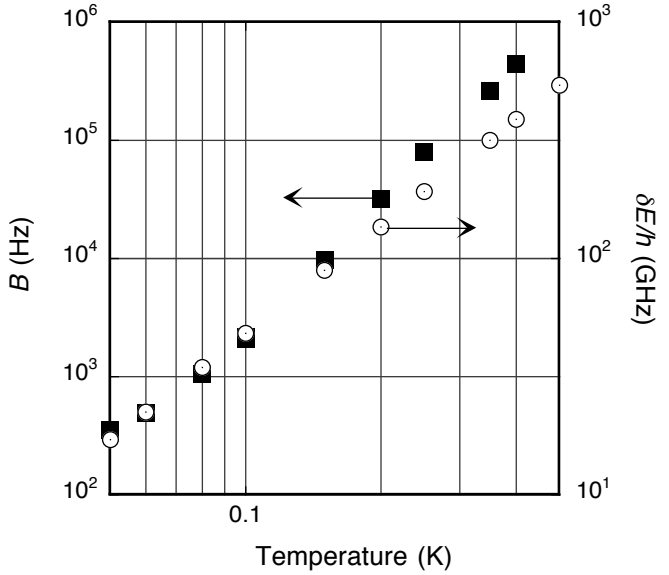

Fig. 2. The expected minimum detectable frequency (red boundary) and the detector system output bandwidth as functions of temperature. At ~ 0.3 K where T_C in *Ti* HEPC is, the red boundary is ~ 170 GHz and the output bandwidth is ~ 100 kHz.

$$NEP_{TEF} = \sqrt{2k_B T_C^2 C_e / \tau_{e-ph}} \qquad (5)$$

Here C_e is the electron heat capacity, $\tau_{e\text{-}ph}$ is the electron-phonon energy relaxation time. NEP_{TEF} can reach 10^{-20} W/Hz$^{1/2}$ for small sensor size at $T \approx 100$ mK [6]. The relaxation time increases with the film disorder and also has a stronger temperature dependence than in a pure metal:

$$\tau_{e-ph} = AT^{-(n-2)} [\mu \text{sec}]. \qquad (6)$$

where $A = 0.4$ for *Hf* and 0.2 for *Ti*, $n = 6$ [13] (in a pure metal, $n = 5$). A record long $\tau_{e\text{-}ph} = 25$ ms has been measured in *Hf* at 40 mK [13] but this is still insufficient for integrating of photons with $N_{ph} \sim 100$ s^{-1}.

IV. Hot-Electron TES Photon Counter

As follows from the above, it will be very difficult if possible at all to realize a combination of the *NEP* $\sim 10^{-20}$ W/Hz$^{1/2}$ and the time constant >> 100 ms. Thus, the photon counting mode for THz radiation becomes unavoidable. Superconducting TES based bolometric photon counters/calorimeters achieving a high energy resolution without using external wavelength dispersing elements have been successfully developed from X-ray to near-IR wavelengths. Their advantages are robust thin-film technology, compatibility with low-noise SQUID readout and the negative electro-thermal feedback improving the energy resolution.

The energy resolution of a calorimeter scales as a square root of the heat capacity of the absorber, therefore very small devices and low temperatures are needed for THz calorimetry. On the other hand, $T \geq 0.3$ K is quite desirable for space applications since this significantly simplifies the cryocooling.

Submicron-size (0.45 μm × 0.17 μm × 0.025 μm) planar antenna-coupled *Ti* HEDD devices have already become available for our work (see Section V). The devices are fabricated on silicon substrates between *Nb* contacts, which will block the diffusion of hot electrons out of the bridge due to Andreev reflection. Further minimization of the device length is limited by the proximity effect: for shorter nanobridges, the superconducting order parameter will propagate from *Nb* contacts in the *Ti* nanobridge and raise its critical temperature. The lower limit on the nanobridge length corresponds to the coherence length in normal metal $L_C = \sqrt{hD/\left(4\pi^2 k_B T\right)} \approx 30$ nm ($D = 2.4$ cm^2/s is the electron diffusivity in *Ti* films). Since L_C is an order of magnitude less then the device length, $L \sim 0.5$ μm, the proximity effect can be neglected.

Here we evaluate the performance of a Hot-Electron Photon Counter (HEPC) in the THz regime. The *Ti* nanobridge will operate in the voltage-biased TES mode with the negative electro-thermal feedback (ETF), that is, its operating temperature will be somewhat lower than the critical temperature, $T_C \approx 300$ mK, and the resistance at the operating point will be much smaller than the normal resistance. An absorbed photon causes a fast increase of the electron temperature in the device, $\delta T_e = h\nu/C_e$, within the characteristic time $\tau_D \approx L^2/\pi^2 D \approx 0.1$ ns. Then the relaxation of electron temperature occurs with the time constant $\tau \approx \tau_{e\text{-}ph} n/\alpha$ ($\alpha \approx 2T_C/\delta T_C$, δT_C is the superconducting transition width). In our previous work [20] with thin–film micron-size *Ti* bridges, $\delta T_C \approx 10$ mK was routinely observed. So $\alpha \sim$ 60-70 is expected to be realized in HEPC devices. The ability of the device to detect single photons depends on the magnitude of the intrinsic thermal fluctuations. The rms energy fluctuation for a TES with strong ETF is given by [21]:

$$\delta E \approx \sqrt{4\sqrt{n/2} k_B T_C^2 C_e / \alpha}\,. \qquad (7)$$

A frequency $\nu_R = \delta E/h = 170$ GHz can be treated as the "red boundary" or the low frequency limit for the detection mechanism. Equation (7) presumes that an optimized filter with the bandwidth $B \approx (2\pi\tau^*)^{-1}$, where $\tau^* = \tau(2/n)^{1/2}$, is used to cut the out-of-band Johnson noise [22].

Both δE and B strongly depend on temperature. In Fig. 2, both temperature dependencies are shown for a *Ti* nanodevice with aforementioned dimensions using experimenatal $\tau_{e\text{-}ph}$ data [13]. Adjusting (reducing) the critical temperature in *Ti* devices, for example, by means of magnetic ion implantation [23] may significantly reduce δE and make detection of THz photons easier. At the same time, the detector bandwidth and its dynamic range will also decrease. The actual trade-off is a matter of several practical cosiderations among which the possibility to operation a detector system in space at 0.3 K instead of 0.1 K stands out as a very important engineering and cost saving factor.

In order to realize the photon-noise limited *NEP*, the dark count rate imposed by the energy fluctuations in the electron subsystem should be below the count rate due to the background radiation. This is achieved by adjusting the discrimination threshold, $E_T < h\nu$, in the photon counter or/and in the readout electronics. Then only the energy

fluctuations, exceeding the discriminator threshold are counted. The corresponding dark count rate is approximately given by [24]:

$$\gamma = \frac{B}{\sqrt{2\pi}} \cdot \int_{E_T/\delta E}^{\infty} \exp\left(-x^2/2\right) dx. \quad (8)$$

The quantum efficiency of the HEPC can be presented as $\eta = \eta_{opt}\eta_{int}$. η_{opt} is the optical coupling efficiency that can be engineered to be close to 100% for a good antenna design. η_{int} is the intrinsic quantum efficiency, that is, a probability of detection after a photon is actually absorbed. This statistical quantity depends on the threshold energy [24]:

$$\eta_{\text{int}} = \frac{1}{\sqrt{2\pi}} \cdot \int_{(E_T - h\nu)/\delta E}^{\infty} \exp\left(-x^2/2\right) dx \quad (9)$$

The result of a numerical modeling of the $NEP = h\nu\sqrt{2\gamma}$ and the quantum efficiency as functions of frequency is shown in Fig. 3. For a higher frequency (1 THz), both low *NEP* (10^{-20} W/Hz$^{1/2}$) and high η_{int} can be readily obtained by adjusting the threshold to $(3\div4)\delta E$. For lower frequencies, the same *NEP* can be obtained only at the expense of the quantum efficiency. Eventually, when $h\nu$ gets close to δE, the optimal E_T approaches zero and the *NEP* approaches that in the integrating mode (~10^{-19} W/Hz$^{1/2}$). Since γ depends very strongly on the lower integration limit (8) it can be varied broadly by choosing E_T or by adjusting the device volume. The latter may be necessary in order to increase the range of frequencies where the counter would operate ($\nu_{max} = C_e\delta T_C/h$).

The value of B determines the maximum count rate and the dynamic range of a counter $10\cdot\log(B/N_{ph}) = 30$-$40$ dB. It is important to understand that the limited device speed is a key condition for keeping the dark count rate low. In another version of the hot-electron bolometric photon counter [25], a normal metal absorber with a normal metal-insulator-superconductor (NIS) thermometer is capacitively coupled to an antenna. In that concept, the thermal relaxation would be governed by the electron diffusion with the characteristic time τ_D ~ ns rather than by the electron-phonon relaxation as in our case. This would result in a very high rate of dark counts exceeding the background photon arrival rate.

Dc SQUIDs with the bandwidth ~ 1 MHz are broadly used for TES readout and are suitable for the HEPC. In future, microwave multiplexed SQUIDs [26] or fully digital RSFQ readouts could be ultimate solutions for the HEPC arrays.

V. Fabrication Procedure and DC Characterization

Currently, we have succeded in fabrication of *Ti* nanodevices with desired dimensions and T_C using *in-situ* e-beam evaporation of *Ti* and *Nb* through a lift-off mask and perfomed some dc tests of the device superconducting properties.

The fabrication process starts with the coating of the substrate (p-type silicon covered with 400 nm of silicon

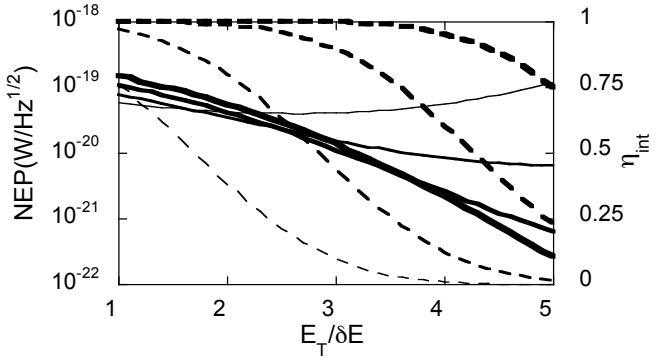

Fig. 3. *NEP* (solid lines) and η_{int} (dashes) as functions of the threshold energy E_T. The optical frequencies are 300 GHz, 500 GHz, 750 GHz, and 1 THz. The line width incrementally increases with the frequency.

oxide) with a double layer of PMGI and PMMA e-beam resist. We have tested several types of the organic shadow masks that can withstand the process of e-gun deposition of *Nb* in the process of multi-angle deposition of the nanoscale HEPCs. These lift-off masks include the top thin PMMA layer, used as a high-resolution electron resist, and the bottom thicker layer that provides a large undercut required for multi-angle deposition through a suspended lift-off mask (see Fig. 4). Our tests showed that the standard PMMA/copolymer masks are incompatible with the e-gun deposition of *Nb* films because of a strong heat-induced outgassing from the mask. The PMGI-based masks compare favorably with the copolymer-based masks because of a higher glass-transition temperature of PMGI (~190^0C).

The device patterning is made using a FEI Sirion SEM and J. C. Nabity's nanometer pattern generation system. After the developing process the samples are mounted in the rotatable stage and in the evaporation chamber.

Our electron-gun evaporation system enables the multi-angle deposition of several (up to four) metals in the same vacuum cycle through the suspended sub-micron mask. The oil-free deposition system is equipped with a cryopump and sorption pumps to avoid possible hydrocarbon contamination. Because of the high melting point of *Nb* ($T = 2468$ C), the electron-gun deposition of superconducting *Nb* films for multi-angle nanopatterning is a non-trivial task: strong radiation from the e-gun source

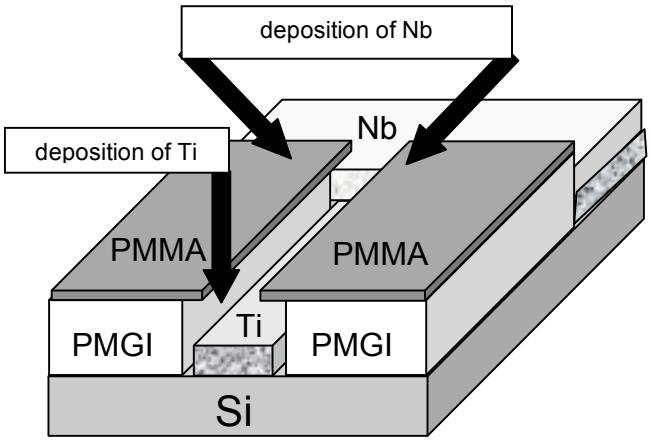

Fig. 4. Illustration of the multi-angle deposition technique. Two layers of resist form a lift-off mask with an overhang protecting *Ti* deposited at 90 deg. into a submicron channel from the following deposition of *Nb* at 45 deg. In the areas much wider than the channel width both layers overlap.

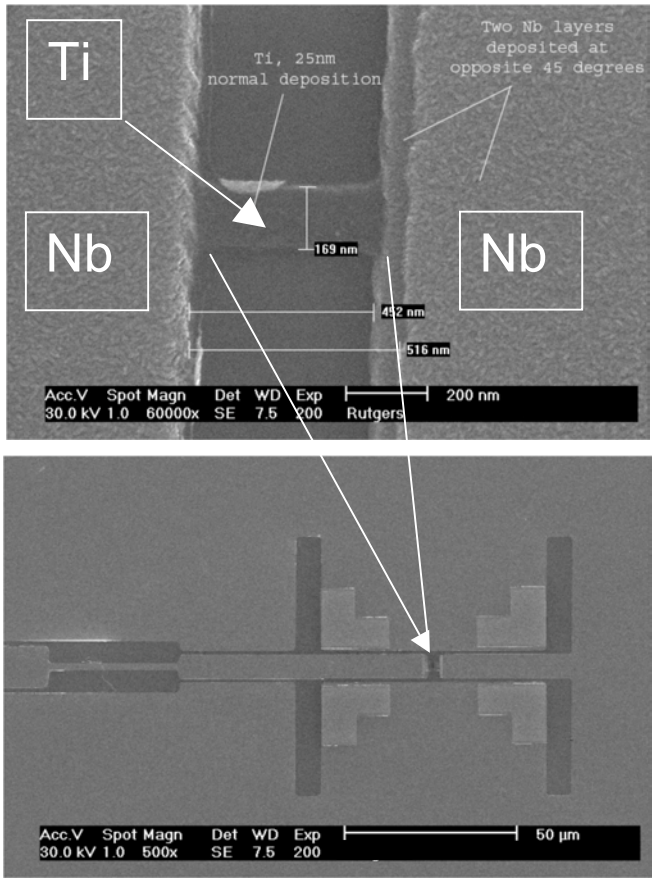

Fig. 5. Upper panel: a 0.45 µm × 0.17 µm *Ti* HEPC device with *Nb* Andreev contacts. Lower panel: an HEPC device integrated into a twin-slot planar antenna centered at 650 GHz.

usually results in compromising the mechanical stability of the PMMA lift-off mask, contamination of the growing *Nb* film with organics, and suppression of superconductivity. To reduce substrate/resist heating, we deposited *Nb* films at an unusually large substrate-to-source distance (~ 37cm). For such a large distance and, hence, a relatively low deposition rate (~ 0.5 nm/sec), the oxidation of growing film becomes a critical issue

To achieve the low pressures needed to obtain clean metal films the chamber is continuously pumped while it is baked for fifteen hours at a temperature of 100 C. At higher temperatures, significant "rounding" of sharp features in the lift-off masks was observed.

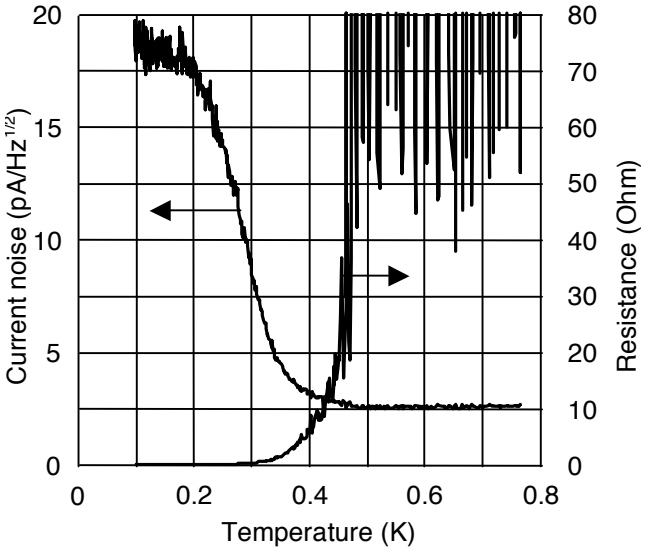

Fig. 6. The temepature dependence of the current noise measured by a SQUID and the corresponding *R(T)* dependence derived from (10). The noise floor above 0.5 K is due to the internal SQUID noise.

During cool down of the chamber the metal sources are outgassed in repeated cycles until small changes in pressure are observed in the process or heating the sources up to the point where we achieve adequate evaporation rates. After cool down, regeneration of the cryopump, and a last outgassing cycle of the sources the base pressure is in the mid 10^{-9} Torr range.

The evaporation of *Ti* and *Nb* is done in a single vacuum cycle to be able to obtain a clean (oxide-free) interface between a *Ti* nanosensor and *Nb* current leads for efficient Andreev confinement of "hot" electrons.

Ti is first deposited at normal incidence to the substrate; the deposition rate is around 0.6 nm per second. During evaporation the pressure in the chamber rises to around 3×10^{-8} Torr. Next, the stage is rotated and *Nb* is deposited at 45 degrees to the substrate and perpendicular to the thin channel. In this way, the thin *Ti* bridge is left uncovered but capped at both ends by *Nb*. A last deposition of *Nb* is done at the opposite 45-degree position to ensure complete covering of the leads. During evaporation of *Nb* the pressure in the chamber will go from about 7×10^{-8} to 3×10^{-7} Torr due to the intense heat radiated from the source. The evaporation rate is 0.5 – 0.6 nm per second. Lift off is done in N-Methyl Pyrrolidione at 95 C followed by rinsing in DI water. An example of the resulting structure is seen in Fig. 5.

Electrical testing of completed HEPC devices represents a significant problem because of the very low power needed to saturate the device, that is, to wash out the superconductivity. This amount can be estimated as $\delta T_C C_e/\tau_{e\text{-}ph} \sim 0.1$ fW. Besides the full enclose of the device into a 0.3 K radiation shield, a properly design low-pass electical filter with cold stages is needed (see, for example, [27]). Such a filter must suppress both low-frequency interferences and rf noise in the range from kHz to several GHz which may overheat the device.

The desing and construction of the filtering system are in progress and, meanwhile, we applied a rather simple SQUID based technique for determining the presence of the superconducting transition in the devices. In this technique, the device is directly connected to the input coil of the dc SQUID without any bias lines. The SQUID senses the device Johnson noise I_{nJ} in the registration bandwidth Δf following the behavior of the device ohmic resistance R:

$$I_{nJ}(T) = \sqrt{4k_B T \Delta f / R(T)}\,. \qquad (10)$$

The available to us SQUID system apparently has strong enough built-in filtering to prevent the HEPC device from overheating by the external noise. An example of the superconducting transition trace for a device similar to that shown in Fig. 5 is demonstrated in Fig. 6. This measurement was done in a dilution refrigerator Kelvinox[25] (Oxford Instruments). The SQUID was situated at a 1.5 K platform so its noise did not depend on the device temperature and remained constant at a level of ≈ 2.5 pA/Hz$^{1/2}$. This sets the limit of sensitivity for this technique and the maximum detectable device resistance was about 50 Ohm. The data clearly demonstrate a superconducting transition above 0.3

K which is similar to what has been observed in larger *Ti* thin-film samples [13,20].

VI. Conclusion

The photon counting detector is important for low-background applications in space THz astronomy where this kind of technology is currently absent. A proposed superconducting HEPC approach is promising for meeting the sensitivity needs while operating at 0.3 K. Beside the astronomical applications, such sensors might be of interest for laboratory molecule spectroscopy, quantum information applications, and nanoscale physics of thermal processes.

References

[1] http://safir.jpl.nasa.gov/technologies/index.asp.

[2] D.J. Benford and S.H. Moseley, "Cryogenic detectors for infrared astronomy: the Single Aperture Far-InfraRed (SAFIR) Observatory," *Nucl. Instr. Meth. Phys. Res. A*, vol. 520, no. 1-3, pp. 379-383, Mar. 2004.

[3] D. Leisawitz, "NASA's far-IR/submillimeter roadmap missions: SAFIR and SPECS," *Adv. Space Res.*, vol. 34, no. 3, pp. 631-636, 2004.

[4] T. Nakagawa, "SPICA: space infrared telescope for cosmology and astrophysics," *Adv. Space Res.*, vol. 34, no. 3, pp. 645-650, 2004.

[5] J.J. Bock, P. Day, A. Goldin, H.G. LeDuc, C. Hunt, A. Lange et al., "Antenna-coupled bolometer array for astrophysics," *Proc. Far-IR, SubMM & MM Detector Technology Workshop, April 1-3, 2002, Monterey, CA*, pp. 224-229.

[6] B.S. Karasik, W.R. McGrath, H.G. LeDuc, and M.E. Gershenson, "A hot-electron direct detector for radioastronomy," *Supercond. Sci. Technol.*, vol. 12, no. 11, pp. 745-747, Nov. 1999; B.S. Karasik, W.R. McGrath, M.E. Gershenson, and A.V. Sergeev, "Photon-noise-limited direct detector based on disorder-controlled electron heating," *J. Appl. Phys.*, vol. 87, no. 10, pp. 7586-7588, May 2000.

[7] A. Vystavkin, D. Chouvaev, L. Kuzmin, M. Tarasov, E. Aderstedt, M. Willander, and T. Claeson, "Andreev reflection based normal metal hot-electron bolometer for space applications", *Proc. SPIE*, vol. 3465, pp. 441-448 (1998).

[8] A.V. Sergeev, V.V. Mitin, and B.S. Karasik, "Ultrasensitive hot-electron kinetic-inductance detectors operating well below superconducting transition", *Appl. Phys. Lett.,* vol. 80, no. 5, pp. 817-819, Feb. 2002.

[9] P.K. Day, H.G. LeDuc, B.A. Mazin, A. Vayonakis, and J. Zmuidzinas, "A broadband superconducting detector suitable for use in large arrays," *Nature*, vol. 425, pp. 817-821, Oct. 2003.

[10] R.J. Schoelkopf S.H. Moseley, C.M. Stahle, P. Wahlgren, and P. Delsing, "A concept for a submillimeter-wave single-photon counter," *IEEE Trans. Appl. Supercond.*, vol. 9, no. 2, Pt. 3, pp. 2935-2939, June 1999.

[11] A. Semenov, A. Engel, K. Il'in, G. Gol'tsman, M. Siegel and H.W. Hubers, "Ultimate performance of a superconducting quantum detector", *Eur. Phys. J. Appl. Phys.*, vol. 21, no. 3, pp. 171-178, Mar. 2003.

[12] S. Komiyama, O. Astafiev, V. Antonov, T. Kutsuwa, and H. Hirai, "A single-photon detector in the far-infrared range," *Nature*, vol. 403, pp. 405-407, Jan. 2000; O. Astafiev, S. Komiyama, T. Kutsuwa, V. Antonov, Y. Kawaguchi, and K. Hirakawa, "Single-photon detector in the microwave range," *Appl. Phys. Lett*, vol. 80, no. 22, pp. 4250-4252, June 2002; H. Hashiba, V. Antonov, L. Kulik, S. Komiyama, and C. Stanley, "Highly sensitive detector for submillimeter wavelength range," *Appl. Phys. Lett.,* vol. 85, no. 24, pp. 6036-6038, Dec. 2004.

[13] M.E. Gershenson, D. Gong, T. Sato, B.S. Karasik, and A.V. Sergeev, "Millisecond Electron-Phonon Relaxation in Ultrathin Disordered Metal Films at Millikelvin Temperatures," *Appl. Phys. Lett.,* vol. 79, no. 13, pp. 2049-2051, Sep. 2001.

[14] M. Yun, J. Beeman, R. Bhatia, J. Bock, W. Holmes, L. Husted et al., "Bolometric Detectors for the Planck Surveyor," *Proc. SPIE,* vol. 4855, pp. 136-147 (2002); W. Holmes, J. Bock, K. Ganga, V.V. Hristov, L. Histead, T. Koch et al., "Preliminary Performance Measurements of Bolometers for the Planck High Frequency Instrument," *Proc. SPIE,* vol. 4855, pp. 208-216 (2002).

[15] L.G.C. Rego and G.Kirczenow, "Quantized thermal conductance of dielectric quantum wires," *Phys. Rev. Lett*., vol. 81, no. 1, pp. 232-235, July 1998.

[16] K. Schwab, E.A. Henriksen, J.M. Worlock, and M.L. Roukes, "Measurement of the quantum of thermal conductance," *Nature,* vol. 404, pp. 974-977, Apr. 2000.

[17] C.S. Yung, D.R. Schmidt, and A.N. Cleland, "Thermal conductance and electron-phonon coupling in mechanically suspended nanostructures," *Appl. Phys. Lett.*, vol. 81, no. 1, pp. 31-33, July 2002.

[18] T. Yamamoto, S. Watanabe, and K. Watanabe, "Universal features of quantized thermal conductance of carbon nanotubes," *Phys. Rev. Lett.*, vol. 92, no. 7, art. no. 075502, Feb. 2004.

[19] C.M. Wilson, L. Frunzio, and D.E. Prober, "Time-Resolving Measurements of Thermodynamic Fluctuations of the Particle Number in a Nondegenerate Fermi Gas," *Phys. Rev. Lett.*, vol. 87, no. 6, art. 067004, Aug. 2001.

[20] B.S. Karasik, B. Delaet, W.R. McGrath, J. Wei, M.E. Gershenson, and A.V. Sergeev, "Experimental Study of Superconducting Hot-Electron Sensors for Submm Astronomy," *IEEE Trans. Appl. Supercond.*, vol. 13, no. 2, Part 1, pp. 188-191, June 2003.

[21] K.D. Irwin, "An application of electrothermal feedback for high resolution cryogenic particle detection," *Appl. Phys. Lett.*, vol. 66, no. 15, pp. 1998-2000, April 1995.

[22] D. McCammon, "Physics of low-temperature microcalorimeters," *Nucl. Instr. Meth. Phys. Res. A*, vol. 520, no. 1-3, pp. 11-15, Mar. 2004.

[23] B.A. Young, J.R. Williams, S.W. Deiker, S.T. Ruggerio, and B. Cabrera, "Using ion implantation to adjust the transition temperature of superconducting films," *Nucl. Instr. & Methods A,* vol. 520, no. 1-3, pp. 307-310, Mar. 2004.

[24] R.H. Kingston, "Detection of Optical and Infrared Radiation," Springer Ser. in Opt. Sci., Ed. D.L. MacAdam, Springer-Verlag, 1978, Ch. 10.

[25] D.V. Anghel and L. Kuzmin, "Capacitively coupled hot-electron nanobolometers as far-infrared photon counter," *Appl. Phys. Lett.*, vol. 82, no. 2, pp. 293-295, Jan. 2003.

[26] K.D. Irwin and K.W. Lehnert, "Microwave SQUID multiplexer," *Appl. Phys. Lett.*, vol. 85, no. 11, pp. 2107-2109, Sep. 2004.

[27] K. Bladh, D. Gunnarson, E. Hürtfled, S. Devi, C. Krisotffersson, B. Smålander, S. Pehrson, T. Claeson, P. Delsing, and M. Taslakov, "Comparison of cryogenic filters for use in single electonics experiments," *Rev. Sci. Instr.,* vol. 74, no. 3, pp. 1323-1327, Mar. 2003.